



1 **Global carbon uptake of cement carbonation accounts 1930-2021**

2 Zi Huang^{1,3*}, Jiaoyue Wang^{2,8,9,*}, Longfei Bing^{2,8,9,*}, Yijiao Qiu¹, Rui Guo¹, Ying
3 Yu⁴, Mingjing Ma², Le Niu², Dan Tong¹, Robbie M. Andrew⁵, Pierre Friedlingstein⁶,
4 Josep G. Canadell⁷, Fengming Xi^{2,8,9}, Zhu Liu¹

5 ¹Department of Earth System Science, Tsinghua University, Beijing 100084, China

6 ²Institute of Applied Ecology, Chinese Academy of Sciences, Shenyang 110016,
7 China

8 ³Department of Engineering Science, University of Oxford, Oxford, OX1 3PJ, UK

9 ⁴Department of Environmental Sciences and Engineering, University of North
10 Carolina at Chapel Hill, Chapel Hill 27599, United States

11 ⁵CICERO Center for International Climate Research, Oslo 0349, Norway

12 ⁶Department of mathematic and statistics, University of Exeter, Exeter, EX4 4QF, UK

13 ⁷CSIRO Environment, Canberra, ACT 2601, Australia

14 ⁸ Key Laboratory of Pollution Ecology and Environmental Engineering, Chinese
15 Academy of Sciences, Shenyang 110016, China

16 ⁹Key Laboratory of Terrestrial Ecosystem Carbon Neutrality, Liaoning Province,
17 China

18 *These authors contributed equally to this work.

19 Correspondence: Fengming Xi (xifengming@iae.ac.cn) and Zhu Liu
20 (zhuliu@tsinghua.edu.cn)

21 **Abstract:**

22 The main contributor to the GHG footprint of the cement industry is the
23 decomposition of alkaline carbonates during clinker production. However, systematic
24 accounts for the reverse of this process - namely carbonation of calcium oxide and other
25 alkaline oxides/hydroxides within cement materials during cements' life cycle have
26 only recently been undertaken. Here, adopting a comprehensive analytical model, we



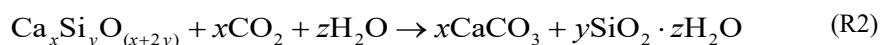
27 provide the most updated estimates of CO₂ uptake by cement carbonation. The
28 accumulated amount of global CO₂ uptake by cements produced from 1930 to 2021 is
29 estimated to be 22.9 Gt CO₂ (95% Confidence interval, CI: 19.6-26.6 Gt CO₂). This
30 amount includes the CO₂ uptake by concrete, mortar, and construction waste and kiln
31 dust. The cumulative carbon uptake by cement materials from 1930 to 2021 offsets 55.1%
32 of the emissions from cement production (41.6 Gt CO₂, 95% CI: 38.7-47.2 Gt CO₂)
33 over the same period, with the greater part coming from mortar (58.5% of the total
34 uptake). China has the highest cement carbon uptake, with cumulative carbonation of
35 7.06 Gt CO₂ (95% CI: 5.22-9.44 Gt CO₂) since 1930. As a result of rapidly increased
36 production in recent year, over three-quarters of the cement carbon uptake has occurred
37 since 1990. Additionally, our results show little impact of the COVID-19 pandemic on
38 cement production and use, with carbon uptake reaching about 0.92 Gt CO₂ (95% CI:
39 0.78-1.10 Gt CO₂) in 2020 and 0.96 Gt CO₂ (95% CI: 0.81-1.15 Gt CO₂) in 2021. Our
40 uniformly formatted and most updated cement uptake inventories provide coherent data
41 support for including cement carbon uptake into future carbon budgets from the local
42 to global scale. The latest version contains the uptake data till 2021, showing the global
43 uptake increasing pattern and offering more usable and relevant data for evaluating
44 cement's carbon uptake capacity. All the data described in this study are accessible at
45 <https://doi.org/10.5281/zenodo.7516373> (Bing et al., 2023).

46 **1 Introduction**

47 With continued urbanization in the developing world and infrastructure projects
48 worldwide, cement consumption has increased rapidly (Low, 2005). The cement
49 production process is an energy-intensive and CO₂-emitting process, the total CO₂
50 emission of which amounts to 5–8 % of global CO₂ emissions (IEA, 2019; Xuan et al.,
51 2019; Friedlingstein et al. 2022). The worldwide average CO₂ emission coefficient of
52 ordinary Portland cement (OPC) is 0.86 kgCO₂/kg (Damtoft et al., 2008), which
53 comprises the release of 0.53 kgCO₂ /kg of clinker owing to the decomposition of



54 limestone during calcination. While in use, though, cement materials that are exposed
55 to air naturally undergo carbonation (Pade and Guimaraes, 2007; Renforth et al., 2011;
56 Huntzinger et al., 2009), a physicochemical process where atmospheric CO₂ gradually
57 absorbs into concrete's structure and reacts with alkaline components such as CaO in a
58 moist environment. The main carbonation mechanisms that are responsible for the
59 carbon uptake can be attributed to the oxides, hydroxide and silicate constituents, as
60 described by Reactions (R1) and (R2).



61 Unfortunately, from the perspective of offsetting emissions in the production of
62 cement, carbonation is a slow process that occurs over the entire life-cycle of
63 cementitious materials, in contrast to the instantaneous CO₂ emissions during their
64 production (Andersson et al., 2013). It has been shown that up to a quarter of the CO₂
65 emitted in cement production can be reabsorbed throughout a building's life and
66 recovery phase (Xi et al., 2016). Quite a few procedures for evaluating the CO₂ footprint
67 over cement's lifecycle have been suggested (Damineli et al., 2010; Renforth et al.,
68 2011; Yang et al., 2013; Cao et al., 2020). Most procedures, however, consider only a
69 case limited system boundary and material type such as concrete service stage,
70 recycling phase of concrete after demolition (Andersson et al., 2013; Yang et al., 2014;
71 Xi et al., 2016; Cao et al., 2020; Kaliyavaradhan et al., 2020), and do not take other
72 types and stages of the lifecycle into systematic account. In our previous study (Guo et
73 al., 2021), which incorporated the merits from other work (Andersson et al., 2013; Yang
74 et al., 2014; Xi et al., 2016; Cao et al., 2020; Kaliyavaradhan et al., 2020) and the
75 updated clinker ratio and/or cement production data, we constructed a comprehensive
76 analytical model to estimate the time-series of cement CO₂ uptake inventories and
77 estimated that 21.02 Gt CO₂ had been sequestered in cements produced between 1930
78 and 2019, which abated 55% of the corresponding process emission over the same



79 period.

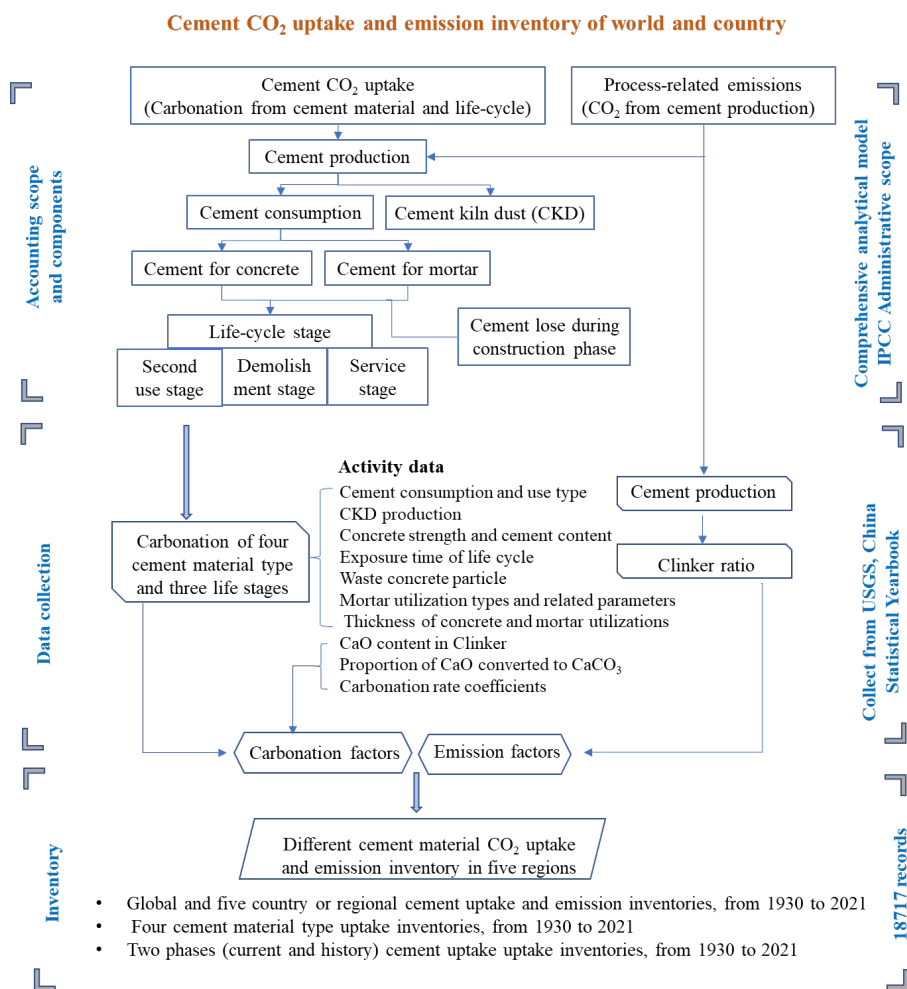
80 The cement CO₂ uptake and emission dataset can be accounted annually. In this study,
81 based on the previous data frameworks (Guo et al., 2021), we updated cement
82 production and emission factors, and most up-to-date clinker ratio data of the year of
83 2020 and 2021. Adopting previous comprehensive analytical model (Guo et al., 2021),
84 we updated the cement CO₂ uptake and emission dataset from 1930 to 2021. The
85 inventories are constructed in a uniform format, which includes cement process-related
86 emissions and cement uptake from four material types with three life stages burned in
87 five countries or regions. The uniformly formatted time-series cement uptake
88 inventories can be utilized widely. Using this consistent framework and models, we
89 provide an updated annual cement carbon uptake to be used in the annual assessments
90 of the global carbon budget (GCB) (Friedlingstein et al., 2022). These timely updated
91 inventories can provide robust data support for further analysis of global or regional
92 emissions reduction policy-making, especially for carbon-intensive industry like
93 cement manufacturing industry. By accelerating carbon capture from existing cement
94 materials and using waste concrete as a carbon storage material, cement could reduce
95 its net carbon emission impact. The primary focus of this research is to update the
96 cement carbon uptake data up to 2021 using a methodology consistent with our previous
97 publication. By doing so, we aim to provide the most current and up-to-date data to
98 accurately portray the impact of cement carbon uptake. The data can be downloaded
99 freely from <https://doi.org/10.5281/zenodo.7516373>.

100 **2 Data and Methods**

101 The cement CO₂ uptake and process emission in this dataset were estimated in terms
102 of the comprehensive analytical model and based on IPCC administrative territorial-
103 based accounting scope. In addition, we also assessed the uncertainties in cement
104 uptake and process emission estimates using the Monte Carlo method that IPCC
105 recommended. The detail input data are in SI-Table 1 (available online only). Our
106 inventories were constructed in two parts: process-related (cement) CO₂ emissions and



107 cement material uptake. Figure 1 presents a diagram of the entire construction of our
 108 cement material carbonation uptake and cement emission inventories.



109
 110 Figure 1. Diagram of cement CO₂ uptake and emission inventory construction.

111 **2.1 Cement production data sources**

112 To keep the consistency with the previous study (Xi et al., 2016; Guo et al., 2021),
 113 we still obtained the global cement production data from 1930 to 2021 from the United
 114 States Geological Survey (USGS) and geographically divided into five primary
 115 countries and aggregated regions, including China, the United States (US), Europe and
 116 central Eurasia (including Russia), India and the rest of the world (ROW). In this study,



117 we updated cement production for year 2020 and 2021, and the global cement
118 production was collected from USGS cement statistics and information annual report
119 (USGS, 2022), regional cement productions were gained from China Statistical
120 Yearbook (NBS, 2022), USGS cement annual publication (USGS, 2022), Trading
121 Economics (2019) for China, the United States (US), Europe and Central Eurasia
122 (including Russia) and India, respectively. The clinker ratio data was kept the same with
123 the previous data sources (CCA et al., 2001-2005; Xu et al., 2012; Xu et al., 2014; Cao
124 et al., 2017; MIIT, 2019) except the US which was collected from USGS annual cement
125 report (USGS, 2022).

126 **2.2 Cement process emission calculation**

127 In producing cement clinker, the major constituent of cement (OPC), limestone
128 together with other carbonates are decomposed into their corresponding oxides and
129 gaseous CO₂ via calcination, resulting in the process emission of the cement industry.
130 It is a so-called hard-to-abate CO₂ emission source (Antunes et al., 2021) because no
131 clear avenue has yet been found to replace this chemical process. Therefore, the process
132 emission intensity (factor) is related to the composition of the clinker and its content in
133 the cements in question. The IPCC recommended default value of process emission
134 factor is 0.507 kg CO₂ kg⁻¹ clinker (EFDB, 2002), without the emissions associated
135 with MgCO₃. In our work, the value of clinker ratio for China was taken to be 0.51966
136 kg CO₂ kg⁻¹ clinker for dry with preheater without pre-calciner, dry with preheater and
137 pre-calciner, and dry without preheater (long dry) kilns, and 0.49983 kg CO₂ kg⁻¹
138 clinker for semi-wet or semi-dry and wet or shaft kilns since 2005, as adapted from
139 Shen's study (Shen et al., 2016). For other countries, Andrew's recent work (Andrew,
140 2019) established a sound foundation for those who are in absence of survey data.
141 Besides, the survey data was obtained from the World Business Council for Sustainable
142 Development (WBCSD) and the Global Cement Directory 2019 (publicly named as the
143 GCD-2019 dataset). Finally, the use of integrated global plant-level capacity and
144 technology information was maintained and continued in this study for higher accuracy



145 in contrast to regionally averaged cement emission factors (Guo et al., 2021).

146 In general, the process emission can be calculated by Equation 1:

$$E_{process,i} = P_{cement,i} \times f_{clinker,i} \times EF_{CO_2,i} \quad (1)$$

147 Where $E_{process,i}$ is the cement process emission of the different regions. $P_{cement,i}$ is
148 the regional cement production. The $f_{clinker,i}$ and $EF_{CO_2,i}$ are clinker to cement ratios
149 and cement (clinker) carbon emission factors of these five regions respectively.

150 2.3 Cement life-cycle uptake assessments

151 The cement utilization was categorized by four types: concrete, mortar, cement kiln
152 dust and cementitious construction wastes, which included three life stages (Xi et al.,
153 2016; Guo et al., 2021) named:(1) service, (2) demolition, and (3) second use. Thus,
154 the whole carbon uptake process can be designed as

$$C_{uptake} = C_{concrete} + C_{mortar} + C_{wastes} + C_{CKD} \quad (2)$$

$$C_{concrete} = C_{l,tl} + C_{d,td} + C_{s,ts} \quad (3)$$

$$C_{mortar} = C_{l,tl} + C_{d,td} + C_{s,ts} \quad (4)$$

155 Where C_{uptake} , $C_{concrete}$, C_{mortar} , and C_{waste} are the uptake amounts of every types. $C_{l,tl}$,
156 $C_{d,td}$, and $C_{s,ts}$ are the uptake amounts during service, demolition and secondary-use
157 stages, respectively. Following our previous study, 100 years were considered to be the
158 total life-cycle time. During service stage, cement materials are mainly used for civil
159 infrastructures' constructions. Based on Fick's second law, a simplified model was
160 applied in this work which introduced a two-dimensional diffusion "slab" process
161 shown in Fig. 2. Fick's second law determines the relationship of carbonization depths
162 and reaction time(tl) linked by diffusion coefficient (k), which can be described as:

$$d = k\sqrt{tl} \quad (5)$$

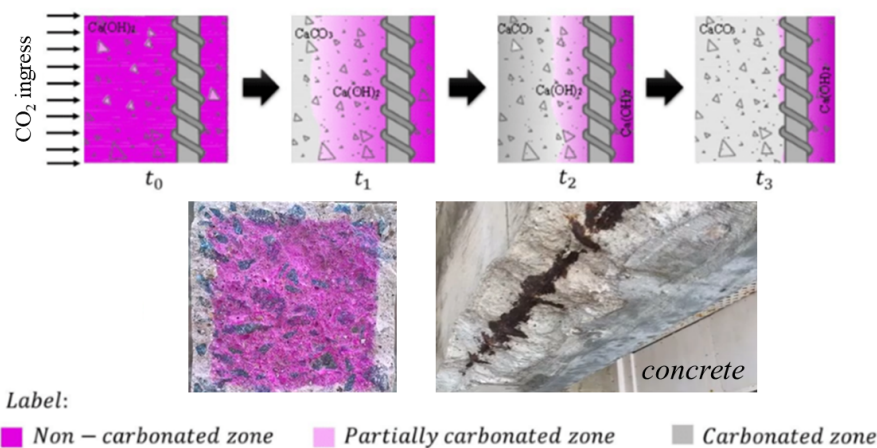
163 Then, based on the reaction of cement carbonation and IPCC's report, the carbonation
164 calculation can be expressed to be

$$C = f_{cement}^{clinker} \times f_{clinker}^{CaO} \times \gamma \times \frac{M_{CO_2}}{M_{CaO}} \quad (6)$$



165 Where the $f_{cement}^{clinker}$ is clinker ratio, $f_{clinker}^{CaO}$ is the CaO content in the clinker, and
 166 γ is the fraction of CaO that could be converted to $CaCO_3$. M_{CO_2} is molar mass of
 167 CO_2 . M_{CaO} is molar mass of CaO.

168 In order to simplify the calculation model, some assumptions were applied in this
 169 study. Firstly, the diffusion front was assumed regarded to be the same as the
 170 carbonation front with the area behind the front was fully carbonated; and then, in the
 171 slab model shown as Fig. 2, the carbonation amounts is determined as a function of
 172 exposed surface area, carbonation depth and the cement content of concrete. Due to the
 173 influence on the carbonation process of exposure condition and materials properties, in
 174 this study, for concrete, a compressive-strength-class breakdown was carried out based
 175 on the regional standards. For mortar, the different kinds of utilization – rendering,
 176 masonry and maintenance were considered most important. Two main exposure
 177 conditions (buried and in open air) were considered, with different carbonation
 178 coefficients. Specifically, carbon sequestration of these four types of cementitious
 179 materials was calculated separately according to the methods described in the following
 180 sections.



181
 182 Fig 2. A schematic representation of carbonation model of concretes.

183 2.3.1 Concrete uptake assessments

184 In service stage, after carbonated coefficients in different environment and the



185 correction factors was set (Lagerblad et al., 2005; Pade and Guimaraes, 2007;
186 Zafeiropoulou et al., 2011; Andersson et al., 2013), the carbonation rate of the different
187 strength class materials was set for further use as shown in equation:

$$k_{ci} = C_{o_{environment}} \times \beta_{ad} \times \beta_{CO_2} \times \beta_{CC} \quad (7)$$

188 Where k_{ci} is the carbonation rate of class i . $C_{o_{environment}}$ is the carbonated
189 coefficients under different environments, usually under air or buried environments.
190 β_{ad} , β_{CO_2} and β_{CC} are cement additives, CO₂ concentration, and coating and cover,
191 respectively.

192 Based on the Fick's second law, then the concrete carbonation depth can be
193 calculated by the following:

$$d_{ci} = k_{ci} \times \sqrt{t} \quad (8)$$

194 Where d_{ci} is the depth which depended on carbonation rate and reaction time till
195 the end of service stage. Furthermore, the carbonated amounts over a certain service
196 time can be described as following:

$$W_{C_{use_i}} = C_{ci} \times \frac{d_{ci}}{Tw} \quad (9)$$

197 Where $W_{C_{use_i}}$ is the mass of carbonated cement used in concrete over a certain period
198 of time during the use stage. C_{ci} is the cement content in class i concrete. Tw is the
199 average thickness of concrete structure.

200

201 Finally, the concrete uptake in service stage can be calculated through equation 5.

202

203 The concrete structures would move to demolition stage when they were end of
204 service as civil infrastructures. Since usually the end of use structure would be crashed
205 into small size particles (Engelsen et al., 2005; Kikuchi et al., 2011). In this study, a
206 simplified model of carbonation in demolition stage is established based on the
207 assumptions that the carbonation starts from the outer surface, moving inwards radially
208 as Fig 3. In this model, the three distinct groups of distributions ($b \leq D_{0i}$, $a \leq D_{0i} < b$, $a > D_{0i}$)
209 were defined according to the maximum diameter (D_{0i}) of a particle when undergo full



210 carbonation in compressive strength class i in the respective range of minimum (a) and
 211 maximum diameters (b). Thus, the calculation can be expressed as follow:

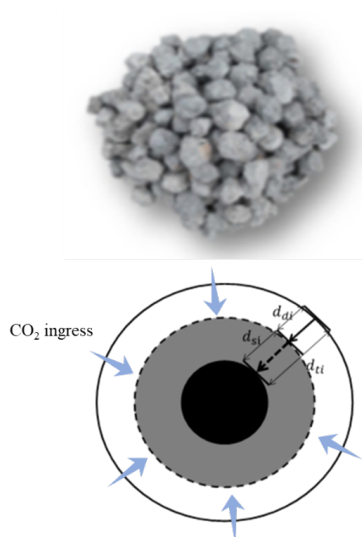
212

$$F_{di} = \begin{cases} 1 - \int_a^b \frac{\pi}{6} (D - D_{0i})^3 / \int_a^b \frac{\pi}{6} D^3 & (a > D_{0i}) \\ 1 - \int_{D_{0i}}^b \frac{\pi}{6} (D - D_{0i})^3 / \int_a^b \frac{\pi}{6} D^3 & (a \leq D_{0i} < b) \\ 1 & (b \leq D_{0i}) \end{cases} \quad (10)$$

$$D_{0i} = 2d_{di} = 2k_{di}\sqrt{t_d} \quad (11)$$

213 Where k_{di} is the diffusion coefficient of compressive strength class i in demolition
 214 stage under “exposed to air” condition. t_d is the subsequent dealing time after service
 215 life. To avoid double counting, the carbonated content in service stage should be
 216 excluded. Thus, the cement uptake in this stage can be calculated as:

$$217 \quad U_{c_{d_i}} = (W_{ci} - W_{c_{use_i}}) \times F_{di} \times f_{cement}^{clinker} \times f_{clinker}^{CaO} \times \gamma \times \frac{M_{CO_2}}{M_{CaO}} \quad (12)$$



White loop is carbonated in demolition stage d_{di} , gray loop is carbonated in secondary use stage d_{si} , and black circle is un-carbonated part, d_{ti} is total carbonation depth in both demolition stage and secondary use stage.

218



219

220 Fig 3. A schematic representation of the spherical carbonation model of a concrete
 221 particle in the demolition stage and second-use stage.

222 Usually, carbonation in the second-use stage is slower because a carbonated layer
 223 has formed out of the particle surface (Yoon et al., 2007; Papadakis et al., 2011). Thus,
 224 a time slag has been considered which was used to modify the equation 8. Then the
 225 carbonated depth in second-use stage is:

$$226 \quad d_{s_{ci}} = \sqrt{k_{d_{ci}} \times \sqrt{t_d} + k_{si} \times \sqrt{t_s}} \quad (13)$$

227 Where $k_{d_{ci}}$ is the carbonation rate of class i concrete during second-use stage. t_d and
 228 t_s are total demolishment time and certain time in second-use stage. Then similar to
 229 demolishment stage, the particle size would affect the carbonation fraction (F_{si}) and
 230 could be calculated as follows:

$$F_{si} = \begin{cases} 1 - \frac{\int_a^b \frac{\pi}{6} (D - D_{ii})^3}{\int_a^b \frac{\pi}{6} D^3} - F_{di} & (a > D_{ii}) \\ 1 - \frac{\int_{D_{ii}}^b \frac{\pi}{6} (D - D_{ii})^3}{\int_a^b \frac{\pi}{6} D^3} - F_{di} & (a \leq D_{ii} < b) \\ 1 & (b \leq D_{ii}) \end{cases} \quad (14)$$

231 Then, the total cement uptake amount in this stage can be expressed as follow:

$$232 \quad U_{C_{s_i}} = (Wc_i - Wc_{use_i} - Wc_{d_i}) \times F_{si} \times f_{cement}^{clinker} \times f_{clinker}^{CaO} \times \gamma \times \frac{M_{CO_2}}{M_{CaO}} \quad (15)$$

233 The factors and values mentioned before vary from different regions based on
 234 surveys.

235 2.3.2 Mortar uptake assessments

236 The mortar utilizations were separated into 3 subcomponents including: (1) rendering
 237 and plastering mortar, (2) masonry mortar, (3) maintenance and repairing mortar
 238 (Winter and Plank, 2007; Xi et al., 2016; Guo et al., 2021). Thus, the total carbon
 239 sequestering of mortar use can be described as below:

$$240 \quad C_{mor} = C_{rpt} + C_{rmt} + C_{rat} \quad (16)$$

241 Where C_{rpt} , C_{rmt} , and C_{rat} are the uptake of the corresponding component,
 242 respectively. Based on our previous experiment results of carbonation diffusion rates



243 (k_m), in this study, k_m was used to replace k_c to establish a two-dimensional diffusion
244 “slab” model, similar to that of concrete. Also, proportion of CaO conversion was
245 updated to gamma 1 (γ_1). In consequence, the carbonation of mortar used for rendering,
246 plastering, and decorating is calculated as follows:

$$d_{rp} = k_m \times \sqrt{t} \quad (17)$$

$$f_{rpt} = \frac{d_{rpt} - d_{rp(t-1)}}{d_{T_{rp}}} \times 100\% \quad (18)$$

$$C_{rpt} = W_m \times r_{rp} \times f_{rpt} \times f_{cement}^{clinker} \times f_{clinker}^{CaO} \times \gamma_1 \times \frac{M_{CO_2}}{M_{CaO}} \quad (19)$$

247 Where d_{rp} is the carbonation depth of rendering mortar. k_m is the carbonation rate
248 coefficient of cement mortar. t is a certain exposure time of rendering mortar after
249 construction. f_{rpt} is the annual carbonation percentage of rendering mortar in year t .
250 $d_{rp,t}$ and $d_{rp,t-1}$ are the carbonation depths of rendering mortar in year t and last year
251 ($t-1$), respectively. $d_{T_{rp}}$ is the thickness for rendering mortar utilization. C_{rpt} is the
252 annual carbon uptake of rendering mortar. W_m is the amount of cement use for mortar.
253 r_{rp} is the use ratio of rendering mortar cement in total mortar cement. γ_1 is the
254 proportion of CaO in mortar cement that fully carbonated to $CaCO_3$.

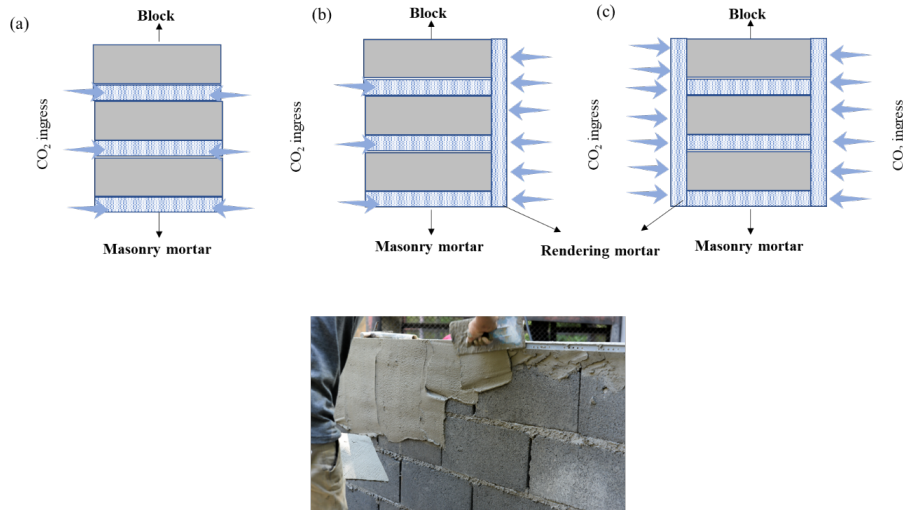
255 Calculation for carbon uptake of repairing and maintaining cement mortar is similar
256 to rendering, plastering, and decorating mortar, with differences in the utilization
257 thickness and the percentage of mortar for repairing and maintaining.

258 Differences were appeared on the calculation of mortar carbon uptake for masonry
259 due to the difference of the partially exposed condition, thicker utilization layers, and
260 their covering by rendering mortar on masonry wall surfaces. Based on surveys, here,
261 the masonry walls were regarded to be three types: walls with both sides rendered (C_{mbr}),
262 walls with one side rendered (C_{mot}), and walls without rendering (C_{mnt}). The main
263 difference is the place of rendering layers on the wall upon the masonry as shown in
264 Fig. 4. Thus, the calculation could be as follows.



$$C_{\text{mat}} = C_{\text{mbt}} + C_{\text{mot}} + C_{\text{mnt}} \quad (20)$$

265 Where C_{mbt} , C_{mot} and C_{mnt} are the uptakes of the above classification, respectively.



266
 267 Fig. 4. A schematic representation of the carbonation model for masonry mortar. (a)
 268 masonry mortar without rendering; (b) masonry mortar with one-side rendering; (c)
 269 masonry mortar with two-side rendering.

270 Here, similar to previous model of carbon uptake in concrete, considering the
 271 carbonation of front rendering, the calculation of carbon uptake of mortar for masonry
 272 is shown below.

$$d_{\text{mb}} = \begin{cases} 0 & (t \leq t_r) \\ 2(K_m \times \sqrt{t} - d_{\text{Trp}}) & (t > t_r) \end{cases} \quad (21)$$

$$f_{\text{mbt}} = \begin{cases} 0 & (t \leq t_r) \\ (d_{\text{mbt}} - d_{\text{mb}(t-1)}) / d_w \times 100\% & (t_r < t \leq t_{sl}) \\ 100\% - d_{\text{mb}t_{sl}} / d_w \times 100\% & (t = t_{sl} + 1) \end{cases} \quad (22)$$

$$C_{\text{mbt}} = W_m \times r_{\text{rm}} \times r_b \times f_{\text{mbt}} \times f_{\text{cement}}^{\text{clinker}} \times f_{\text{clinker}}^{\text{CaO}} \times \gamma_1 \times \frac{M_{\text{CO}_2}}{M_{\text{CaO}}} \quad (23)$$

273 Where d_{mb} is the total carbonation depth of masonry wall with both sides rendered. t
 274 is the exposure time of masonry mortar after construction. t_r is the time used when
 275 rendering mortar full carbonation. d_{Trp} is the thickness of rendering mortar on masonry



276 wall. $f_{m_{bt}}$ is the annual carbonation percentage of masonry mortar with both sides
 277 rendered in year t . $d_{m_{bt}}$ and $d_{m_{b(t-1)}}$ are carbonation depth of masonry mortar with both
 278 sides rendered in year t and $(t - 1)$, respectively. d_w is the thickness of masonry wall. t_{sl}
 279 is the service life of construction. $d_{m_{bt,t}}$ is the carbonation depth of a masonry mortar
 280 with both sides rendered during service life. $C_{m_{bt}}$ is the annual carbon uptake of
 281 masonry mortar with both sides rendered in year t . $r_{m_{bt}}$ is the ratio of cement use for
 282 masonry mortar in total mortar cement. r_b is the ratio of masonry mortar with both sides
 283 rendered in total masonry mortar.

284 2.3.3 Construction wastes uptake assessments

285 Cement wastes account for 1~3% of total cement consumption based on construction
 286 budget standards and survey data (Zhou, 2003; Lu et al., 2011). The main compenence
 287 is concrete waste (45%) and mortar waste (55%) separately (Bossink et al., 1996;
 288 Huang et al., 2013). Thus, in this calculation, they would be considered individually, as
 289 shown below.

$$290 \quad C_{waste} = C_{wastecon} + C_{wastemor} \quad (24)$$

291 Where $C_{wastecon}$ and $C_{wastemor}$ are the uptakes of concrete waste and mortar waste,
 292 respectively. Then, the construction wastes carbonation can be calculated as follow:

$$C_{wastecon} = \left(\sum_1^n W_{ci} \times f_{con} \times r_{con} \right) \times f_{cement}^{clinker} \times f_{clinker}^{CaO} \times \gamma \times \frac{M_{CO_2}}{M_{CaO}} \quad (25)$$

$$C_{wastemor} = \left(\sum_1^n W_{mi} \times f_{mor} \times r_{mor} \right) \times f_{cement}^{clinker} \times f_{clinker}^{CaO} \times \gamma_1 \times \frac{M_{CO_2}}{M_{CaO}} \quad (26)$$

293 Where W_{ci} is the cement used for concrete in strength class i . f_{con} is the loss rate
 294 of concrete cement during construction stage. r_{con} is the annual carbon uptake of
 295 waste concrete during construction stage. W_{mi} is the cement used for mortar in
 296 strength class i , f_{mor} is the loss rate of mortar cement. r_{mor} is the annual carbon
 297 uptake of waste mortar during construction stage.

298 2.3.4 Cement kiln dust (CKD) uptake assessments

299 CKD as the main by-product in cement manufacturing industry was mainly treated



300 as landfilled waste (USEPA, 1993; Khanna, 2003). In this work, its carbonation can be
301 calculated as below.

$$302 \quad C_{CKD} = W_{cem} \times r_{CKD} \times r_{landfill} \times f_{cement}^{clinker} \times f_{CKD}^{CaO} \times \gamma_2 \times \frac{M_{CO_2}}{M_{CaO}} \quad (27)$$

303 Where W_{cem} is the cement production. r_{CKD} is the CKD generation rate when clinker
304 production. $r_{landfill}$ is the ratio of CKD treated to landfill. f_{CKD}^{CaO} is the proportion of
305 CaO in CKD (Siriwardena et al., 2015). γ_2 is the percentage of CaO in CKD that fully
306 carbonated to $CaCO_3$. Additionally, due to its rapid carbonation, this equation is single
307 year calculation.

308 **2.3.5 Uncertainty analysis**

309 Based on Monte Carlo simulation, in this study, the uncertainty estimations are
310 applied in cement process carbon emission and cement carbon uptake models separately.
311 The uncertainty ranges of cement process emission and carbon uptake are in SI-Table
312 4 (Bing et al., 2023). The previous works (Xi et al., 2016) have illustrated the sources
313 of uncertainties. Coherently to previous studies (Xi et al., 2016; Guo et al., 2021), the
314 annual global cement carbon uptake and emission was obtained from regional or
315 material use aggregation, which include 26 variables and factors, shown as SI-Table 2
316 (Bing et al., 2022). Notably, the annual median at a higher level is not equal to the sum
317 of its sublevel components when evaluate the carbon uptake at each level due to the
318 different statistics based on the Monte Carlo simulation results (see
319 <https://doi.org/10.5281/zenodo.7516373>; Bing et al., 2023; Guo et al., 2021). In this
320 work for our model used for 2020 and 2021, most of the distributions and their features
321 of variables remain and refer to the previous estimation. But, the clinker to cement ratio
322 of US is updated based on USGS cement annual report of 2021, leading to a change
323 that the random errors are within the range of $\pm 5\%$ (a uniform distribution).

324 **3 Results and discussions**

325 **3.1 Global and regional CO₂ emissions from cement process**

326 Although, carbon reduction policies have become more stringent and technologies

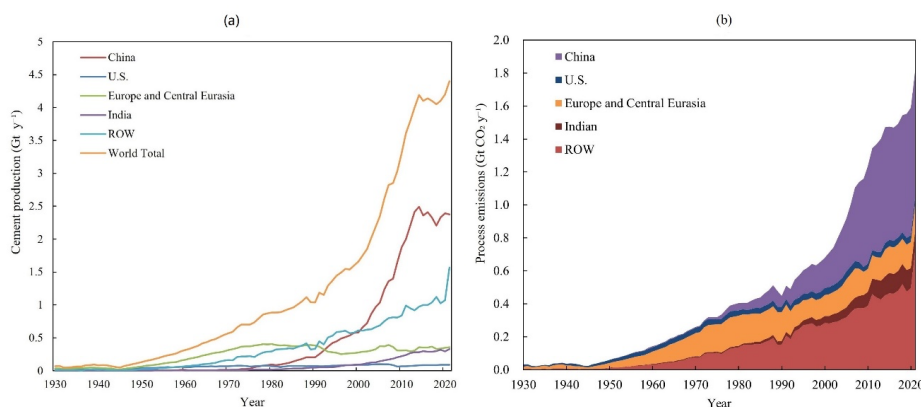


327 more effective since 2019 and accompanied by uncertainties factors that the Covid-19
328 occurred, global CO₂ emissions from cement processes have been increasing rapidly
329 over the recent past decades due to the continuous growth in the production of cement
330 and related clinker as well, but showing a slightly lower average annual growth rate of
331 2019 (8.57%) than that of recent past decades (8.68%). According to our calculations
332 and estimates, the global cement process CO₂ emissions have increased from 0.03 Gt
333 yr⁻¹ in 1930 to 1.81 Gt yr⁻¹ in 2021. Over the period 1930-2021, global cumulative
334 cement process CO₂ emissions amounted to 41.55Gt (95% CI: 38.74-47.19 Gt CO₂), of
335 which ~67% was since 1990, little fewer than that of 2019 (71%). This illustrates that
336 the rapid increase in cement process emissions is mainly driven by industrialization and
337 urbanization accompanied by the development of the global economy. From 1930 to
338 2021, global cement production increased over 6000%, while the growth rate of CO₂
339 emissions (5547.31%) was slightly lower than that of cement production, partly due to
340 the relative decreases in average clinker ratios from ~89 % in 1930 to ~70 % in 2019.
341 (Wang et al., 2021).

342 The regional contribution of CO₂ emissions from the cement process has been altered
343 over the period 1930-2021. As shown in Fig. 5, the CO₂ emissions from the cement
344 process in each region show an overall growth trend, while the growth rate varies by
345 country and region. Among all regions, China experienced the most dramatic increasing
346 emission trend with an annual growth rate of 7.7% and reached 0.76Gt CO₂ (95%
347 CI:0.73-0.80Gt CO₂) in 2021. China contributed 33.5% of cumulative process
348 emissions (13.91Gt CO₂, 95% CI:12.44-17.00 Gt CO₂) during the period 1930-2021.
349 Meanwhile, ROW (mainly developing countries/regions), Europe, and the US were
350 responsible for about 35.6% (14.78Gt CO₂, 95% CI:13.17-17.87 Gt CO₂), 23.98% (9.96
351 Gt CO₂, 95% CI:8.71-12.46 Gt CO₂), and 6.3% (2.62Gt CO₂, 95% CI:2.29-3.27 Gt CO₂)
352 of total cumulative emissions, respectively. India has experienced an incremental
353 growth trend in recent years, totally emitting 2.56 Gt CO₂ (95% CI:2.33-3.02 Gt CO₂),
354 accounting for around 6.2% of process emissions. China and ROW kept their absolute



355 leader role in cement CO₂ emissions till 2021, but the share of India has decreased
356 significantly from ~10% to 6.2% in recent 2 years, partly because of shrink of the
357 cement market during Covid pandemic (Schlorke et al., 2020).



358

359 Fig. 5 Regional and global cement production (a) and process emissions (b) from 1930
360 to 2021

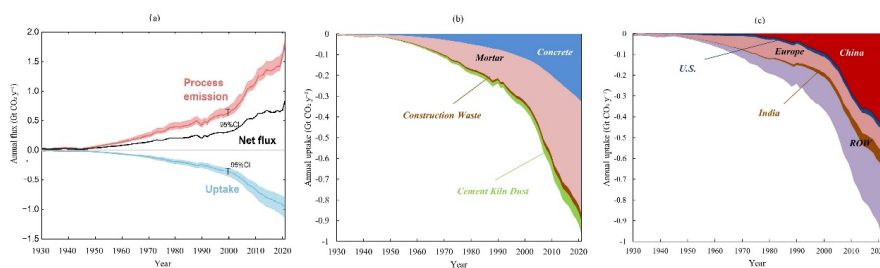
361 3.2 Cement carbon uptake by region and material type

362 According to our estimates, the total global CO₂ uptake by cement reached 0.96 Gt
363 CO₂ (95% CI: 0.81-1.15 Gt CO₂) in 2021, with an average annual growth rate of 7.9%.
364 This means that 30.8% of CO₂ emission from the cement process in 2021 was offset by
365 cement carbon uptake in that year. Global cumulative CO₂ uptake by cement was
366 estimated to be 22.90 Gt CO₂ (95% CI: 19.64-26.64 Gt CO₂), equivalent to ~55% of
367 the cumulative emissions over the same period. As we can see in Fig. 6, in China,
368 cement carbon uptake has increased from 0.05 Mt in 1930 to 426.77 Mt in 2021; its
369 cumulative uptake has reached 7.06 Gt CO₂ (95% CI: 5.22-9.44 Gt CO₂), accounting
370 for 30.8% of global cumulative uptake. The cement carbon uptake in China was
371 growing exponentially, while the growth curves in the US and European countries were
372 relatively smooth. This is mainly because the cement demand in China has observed a
373 rapid growth in recent decades, while developed countries have been close to saturation
374 after the 1980s. Moreover, concrete structures in developed countries have a longer
375 service life (estimated 70 years). As for the rest of world, the total carbon uptake by



376 cement has also increased significantly (from 0.74 Mt in 1930 to 328.23 Mt in 2021),
377 and the growth trend in these countries was smoother than in China but more dramatic
378 than in the US and Europe.

379 In addition, the amount of cement carbon uptake varies depending on the type of
380 cement material. Mortar contributes the largest portion of cement carbon uptake
381 although its application scale is much less than concrete (~73% for concrete use and
382 ~24% for mortar use). This is because mortar, as a building decoration material, has the
383 characteristics of small thickness, large exposed surface area, and therefore fast
384 carbonation kinetics. According to Fig.6, in 2021, the carbon uptake by mortar and
385 concrete were 536.85 Mt and 325.95 Mt, accounting for 55.6% and 33.8% of the total
386 cement carbon uptake, respectively. Meanwhile, CKD and loss waste absorbed 62.60
387 Mt (6.5%) and 34.97 Mt (3.6%) CO₂, respectively.



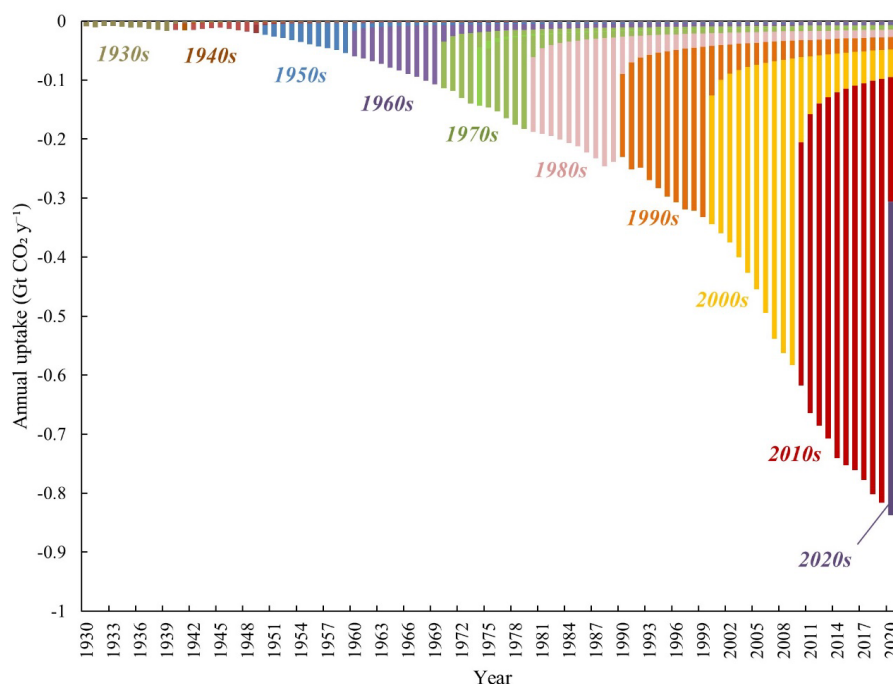
388
389
390 Fig. 6 Annual cement carbon uptake induced net emission (a) and cement CO₂ uptake
391 by different cement materials (b) and by different country or region (c) from 1930 to
392 2021

393 3.3 Features of cement carbon uptake

394 The natural carbonation of cement materials is a slowly dynamic process and thus
395 the carbon uptake by cement has obvious time lag effects. As shown in Fig.7, part of
396 carbon uptake in a given period was contributed by cement materials in previous
397 periods. This is because the cementitious materials carbon uptake is very slow process,
398 leading to a long time to accumulate to manifest and during the demolition period
399 of cement materials, crushing increases its newly exposed surface area and carbonation



400 rate, allowing the carbon uptake capacity of cement materials to persist for a long time.
401 With this feature, the cement carbon uptake capacity can be affected by the service life
402 of cement buildings, and the average lifetime in China (40 years) is less than in the US
403 and Europe (65~75 years). Therefore, countries such as China with a higher speed of
404 cement carbonation cycle can make relatively greater contributions to cement carbon
405 uptake. However, the majority of cement carbon uptake was still attributed to the
406 consumption use stage, providing ~64% share in 2021.



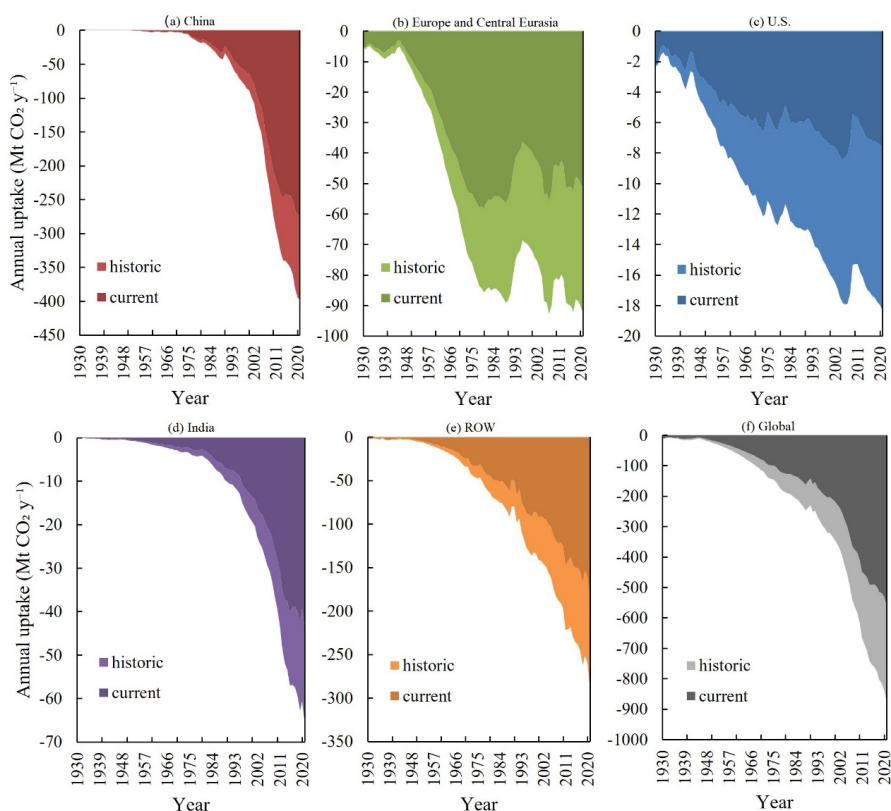
407
408 Fig. 7 The cumulative characteristic of cement carbon uptake. The colour-coded bar
409 areas represent the amount of uptake by the cement produced/consumed in each decade
410 from 1930 to 2021. The fractions of uptake that occurred in each decade post-1990 are
411 annotated. The “tails” indicate that cement produced in a certain time will keep
412 absorbing CO₂ beyond its consumption use stage, and the annual uptakes are composed
413 of current and historical contributions.

414 We can also learn from Fig.8 that the growth rate of historical carbon uptake spiked
415 after the 1990s. It is noteworthy that 75.4% of the cement carbon uptake has occurred



416 since the 1990s, larger than that of 2019 (71%). This surge can be explained by the
417 surplus absorption in the demolition phase due to the historically produced cement in
418 European countries during the 1930s and 1940s, on the one hand, and by the
419 considerably increased demand for cement materials in China after the implementation
420 of the reform and opening-up policy, on the other hand.

421 Besides, the offset level (55.1%) is slightly higher than our previous estimate for
422 1930-2019 (~52%) (Guo et al., 2021), mainly due to the rapid increase demands from
423 ROW during covid pandemic (Schlorke et al., 2020).



424

425 Fig. 8 Annual cement carbon uptake by cement material and region

426 4. Data availability

427 All the original datasets used for estimating the emission and uptake in this study and
428 the resulting datasets themselves from the simulation as well as the associated



429 uncertainties are made available by Zenodo at <https://doi.org/10.5281/zenodo.7516373>
430 (Bing et al., 2023).

431 **5. Conclusions**

432 Due to the unique characteristics of carbon uptake by cement, it is imperative to
433 conduct a scientific and comprehensive estimation of cement carbon uptake. This is
434 crucial for accurately assessing the environmental impact of the cement industry and
435 supporting global carbon neutrality goals. From a kinetic standpoint, cement carbon
436 uptake is a dynamic process that occurs during various stages, including
437 production/consumption, demolition, and reuse. Therefore, it is highly significant to
438 incorporate historical cement legacy sequestration and utilize dynamic clinker ratios to
439 enhance the comprehensiveness and accuracy of estimation. Our objective in this study
440 is to update our data in the temporal dimension, while maintaining consistency with our
441 previous work in terms of methodology. Updating the data within the same framework
442 will enhance the completeness of our database, thereby providing a reliable data
443 foundation for our future forecasting endeavours.

444

445 Based on our estimations, the cumulative carbon uptake by cement materials from
446 1930 to 2021 amounts to 22.90 Gt CO₂ (with a 95% Confidence Interval, CI: 19.64-
447 26.64 Gt CO₂). Mortar contributes approximately 58.5% of the total uptake, effectively
448 offsetting 55.1% of the cumulative process emissions.

449

450 This dataset and estimation methodology can be employed as a valuable set of tools
451 for evaluating cement carbon emissions and uptake throughout the dynamic processes
452 encompassing the entire cement life cycle. While per capita cement stocks in Europe
453 and the United States are reaching saturation levels, China has emerged as the dominant
454 region in cement production and consumption following the implementation of China's
455 reform and opening-up policy. Considering that cement demand in China and other
456 developing countries is expected to continue increasing, it becomes evident that this



457 trend will impact the assessment of global carbon neutrality. Therefore, it is crucial to
458 make further efforts to improve the accuracy of cement carbon uptake estimation by
459 incorporating direct clinker production data and experimentally derived spatially
460 resolved conversion factors.

461

462 **Author contributions**

463 Zi Huang prepared, reviewed, and edited the manuscript with assistance from Jiaoyue
464 Wang, Yijiao Qiu, Longfei Bing, Ying Yu, Rui Guo, Mingjing Ma, Le Niu, Zhu Liu and
465 Fengming Xi. Zi Huang performed the analyses with support from Jiaoyue Wang,
466 Mingjing Ma, Le Niu and Ying Yu on analytical approaches and figure making. Zi
467 Huang, Jiaoyue Wang, and Longfei Bing, Yijiao Qiu curated the datasets. Longfei Bing,
468 Fengming Xi and Zi Huang developed the code and performed the simulations with
469 support from Yijiao Qiu. Dan Tong, Robbie M. Andrew, Pierre Friedlingstein and Josep
470 G. Canadell reviewed, and edited the manuscript. Zhu Liu and Fengming Xi
471 conceptualised and supervised the study.

472 **Competing interests**

473 The authors declare that they have no conflict of interest.

474 **Acknowledgements**

475 Jiaoyue Wang and Fengming Xi acknowledge funding from the Youth Innovation
476 Promotion Association, Chinese Academy of Sciences (2020201 and Y202050), the
477 Natural Science Foundation of China (41977290), Liaoning Xingliao Talents Project
478 (XLYC1907148), Major Program of Institute of Applied Ecology, Chinese Academy of
479 Sciences (IAEMP202201). JGC thanks the support of the National Environmental
480 Science Program – Climate Systems hub.

481

482 **Financial support**

483 This work was supported by the Youth Innovation Promotion Association, Chinese
484 Academy of Sciences (2020201 and Y202050), the Natural Science Foundation of



485 China (41977290), Liaoning Xingliao Talents Project (XLYC1907148), Major Program
486 of Institute of Applied Ecology, Chinese Academy of Sciences (IAEMP202201).

487 **References**

488 Andersson, R., Fridh, K., Stripple, H., and Häglund, M.: Calculating CO₂ Uptake for
489 Existing Concrete Structures during and after Service Life, *Environ. Sci. Tech. Let.*,
490 47, 11625–11633, <https://doi.org/10.1021/es401775w>, 2013.

491 Andrew, R.: Global CO₂ emissions from cement production, 1928–2017, *Earth Syst.*
492 *Sci. Data*, 10, 2213–2239, <https://doi.org/10.5194/essd-10-2213-2018>, 2018.

493 Andrew, R.: Global CO₂ emissions from cement production, 1928–2018, *Earth Syst.*
494 *Sci. Data*, 11, 1675–1710, <https://doi.org/10.5194/essd-11-1675-2019>, 2019.

495 Antunes, M., Santos, R. L., Pereira, J., Rocha, P., Horta, R. B., and Colaço, R.:
496 Alternative Clinker Technologies for Reducing Carbon Emissions in Cement
497 Industry: A Critical Review, *Materials*, 15, 209,
498 <https://doi.org/10.3390/ma15010209>, 2021.

499 Bossink, B. A. G. and Brouwers, H. J. H.: Construction Waste: Quantification and
500 Source Evaluation, *J Constr Eng Manag-ASCE*, 122, 55, 1996.

501 Bing, L. F., Huang, H., Wang, J. Y., Xi, F. M.: Global carbon uptake of cement
502 carbonization accounts 1930-2021, Zenodo[data set],
503 <https://doi.org/10.5281/zenodo.7516373>, 2023.

504 Cao, Z., Myers, R. J., Lupton, R. C., Duan, H., Sacchi, R., Zhou, N., Miller, T. R.,
505 Cullen, J. M., Ge, Q., and Liu, G.: The sponge effect and carbon emission
506 mitigation potentials of the global cement cycle, *Nat. Commun.*, 11, 3777,
507 <https://doi.org/10.1038/s41467-020-17583-w>, 2020.

508 Cao, Z., Shen, L., Løvik, A. N., Müller, D. B., and Liu, G.: Elaborating the History of
509 Our Cementing Societies: An in-Use Stock Perspective, *Environ. Sci. Tech. Let.*,
510 51, 11468–11475, <https://doi.org/10.1021/acs.est.7b03077>, 2017.

511 China Cement Association (CCA): China Cement Almanac, China Building Industry
512 Press, Beijing, China, 2001–2015.



- 513 Damineli, B. L., Kemeid, F. M., Aguiar, P. S., and John, V. M.: Measuring the eco-
514 efficiency of cement use, *Cement Concrete Comp.*, 32, 555–562,
515 <https://doi.org/10.1016/j.cemconcomp.2010.07.009>, 2010.
- 516 Damtoft, J. S., Lukasik, J., Herfort, D., Sorrentino, D., and Gartner, E. M.: Sustainable
517 development and climate change initiatives, *Cement Concrete Res.*, 38, 115–127,
518 <https://doi.org/10.1016/j.cemconres.2007.09.008>, 2008.
- 519 EFDB: Emission Factor for CO₂ Emissions from Cement Production, available at:
520 https://www.ipcc-nggip.iges.or.jp/EFDB/ef_detail.php, 2002.
- 521 Friedlingstein, P., Jones, M. W., O’Sullivan, M., Anew, R. M., Bakker, D. C. E., Hauck,
522 J., Quéré, C. L., Peters, G. P., Peters, W., Pongratz, J., Sitch, S., Canadell, J. G.,
523 Ciais, P., Jackson, R. B., Alin, S. R., Anthoni, P., Bates, N. R., Becker, M., Bellouin,
524 N., Bopp, L., Chau, T. T. T., Chevallier, F., Chini, L. P., Cronin, M., Currie, K. I.,
525 Decharme, B., Djeutchouang, L. M., Dou, X., Evans, W., Feely, R. A., Feng, L.,
526 Gasser, T., Gilfillan, D., Gkritzalis, T., Grassi, G., Gregor, L., Gruber, N., Gürses,
527 Ö., Harris, I., Houghton, R. A., Hurtt, G. C., Iida, Y., Ilyina, T., Luijkx, I. T., Jain,
528 A., Jones, S. D., Kato, E., Kennedy, D., Goldewijk, K. K., Knauer, J., Korsbakken,
529 J. I., Körtzinger, A., Landschützer, P., Lauvset, S. K., Lefèvre, N., Lienert, S., Liu,
530 J., Marland, G., McGuire, P. C., Melton, J. R., Munro, D. R., Nabel, J. E. M. S.,
531 Nakaoka, S. I., Niwa, Y., Ono, T., Pierrot, D., Poulter, B., Rehder, G., Resplandy,
532 L., Robertson, E., Rödenbeck, C., Rosan, T. M., Schwinger, J., Schwingshackl, C.,
533 Séférian, R., Sutton, A. J., Sweeney, C., Tanhua, T., Tans, P. P., Tian, H., Tilbrook,
534 B., Tubiello, F., Werf, G. R. V. D., Vuichard, N., Wada, C., Wanninkhof, R., Watson,
535 A. J., Willis, D., Wiltshire, A. J., Yuan, W., Yue, C., Yue, X., Zaehle, S., and Zeng,
536 J.: Global Carbon Budget 2021, *Earth Syst. Sci. Data*, 14, 1917–2005,
537 <https://doi.org/10.5194/essd-14-1917-2022>, 2022.
- 538 Global Cement Directory: Global Cement Directory - listing of all global cement plants
539 from Global Cement, available at: <https://www.globalcement.com/directory>, 2019
- 540 Guo, R., Wang, J., Bing, L., Tong, D., Ciais, P., Davis, S., Andrew, R., Xi, F., and Liu,



- 541 Z.: Global CO₂ uptake by cement from 1930 to 2019, *Earth Syst. Sci. Data*, 13,
542 1791–1805, <https://doi.org/10.5194/essd-13-1791-2021>, 2021.
- 543 Huang, T., Shi, F., Tanikawa, H., Fei, J., and Han, J.: Materials demand and
544 environmental impact of buildings construction and demolition in China based on
545 dynamic material flow analysis, *Resour. Conserv. Recy.*, 72, 91–101,
546 <https://doi.org/10.1016/j.resconrec.2012.12.013>, 2013.
- 547 Huntzinger, D. N., Gierke, J. S., Kawatra, S. K., Eisele, T. C., and Sutter, L. L.: Carbon
548 Dioxide Sequestration in Cement Kiln Dust through Mineral Carbonation, *Environ.*
549 *Sci. Tech. Let.*, 43, 1986–1992, <https://doi.org/10.1021/es802910z>, 2009.
- 550 IEA: CO₂ Emissions from Fuel Combustion 2019, International Energy Agency,
551 <https://doi.org/10.1787/9789264096134-en>, 2019.
- 552 Kaliyavaradhan, S. K., Ling, T.-C., and Mo, K. H.: CO₂ sequestration of fresh concrete
553 slurry waste: Optimization of CO₂ uptake and feasible use as a potential cement
554 binder, *J. CO₂ Util.*, 42, 101330, <https://doi.org/10.1016/j.jcou.2020.101330>,
555 2020.
- 556 Khanna, O.: Characterization and utilization of cement kiln dusts (CKDs) as partial
557 replacements of Portland cement, 344 pp., 2009.
- 558 Kikuchi, T. and Kuroda, Y.: Carbon Dioxide Uptake in Demolished and Crushed
559 Concrete, *J. Adv. Concr. Technol.*, 9, 115–124, <https://doi.org/10.3151/jact.9.115>,
560 2011a.
- 561 Kikuchi, T. and Kuroda, Y.: Carbon Dioxide Uptake in Demolished and Crushed
562 Concrete, *J. Adv. Concr. Technol.*, 9, 115–124, <https://doi.org/10.3151/jact.9.115>,
563 2011b.
- 564 Lagerblad, B.: Carbon Dioxide Uptake during Concrete Life Cycle - State of the Art,
565 Cement och Betong Institutet, Stockholm, 47 pp., 2005.
- 566 Longfei, B., Zi, H., Jiaoyue, W., and Fengming, X.: Global carbon uptake of cement
567 carbonization accounts 1930-2021, , 1, <https://doi.org/10.5281/zenodo.7516373>,
568 [2022](https://doi.org/10.5281/zenodo.7516373), 2023.



- 569 Low, M.-S.: Material flow analysis of concrete in the United States, S.M., Department
570 of Architecture, Massachusetts Institute of Technology, USA,
571 <http://hdl.handle.net/1721.1/33030>, 2005.
- 572 Lu, W., Yuan, H., Li, J., Hao, J. J. L., Mi, X., and Ding, Z.: An empirical investigation
573 of construction and demolition waste generation rates in Shenzhen city, South
574 China, *Waste Manag.*, 31, 680–687,
575 <https://doi.org/10.1016/j.wasman.2010.12.004>, 2011.
- 576 MIT: Building
577 materials, <http://www.mit.gov.cn/n1146312/n1146904/n1648356/n1648361/index.html>,
578 last access: 22 August 2020, 2019
- 579 NBS: National data, available at: <https://data.stats.gov.cn/> (last access: 22 August 2020),
580 2019.
- 581 Pade, C. and Guimaraes, M.: The CO₂ uptake of concrete in a 100 year perspective,
582 *Cement. Concrete. Res.*, 37, 1348–1356,
583 <https://doi.org/10.1016/j.cemconres.2007.06.009>, 2007.
- 584 Papadakis, V. G., Vayenas, C. G., and Fardis, M. N.: Experimental investigation and
585 mathematical modeling of the concrete carbonation problem, *Chem. Eng. Sci.*, 46,
586 1333–1338, [https://doi.org/10.1016/0009-2509\(91\)85060-B](https://doi.org/10.1016/0009-2509(91)85060-B), 1991.
- 587 Renforth, P., Washbourne, C.-L., Taylder, J., and Manning, D. A. C.: Silicate Production
588 and Availability for Mineral Carbonation, *Environ. Sci. Tech. Let.*, 45, 2035–2041,
589 <https://doi.org/10.1021/es103241w>, 2011.
- 590 Schlorke, S., Tu, L., Stec, M., Mallagray, J. V., and Kaleem, H.: The Impact of COVID-
591 19 on the Cement Industry, International Finance Corporation, Washington, DC,
592 2020.
- 593 Shen, L., Zhao, J., Wang, L., Liu, L., Wang, Y., Yao, Y., Geng, Y., Gao, T., and Cao, Z.:
594 Calculation and evaluation on carbon emission factor of cement production in
595 China, *Chinese Sci. Bull.*, 61, 2926–2938, <https://doi.org/10.1360/N972016-00037>,
596 2016.



- 597 Siriwardena, D. P. and Peethamparan, S.: Quantification of CO₂ sequestration capacity
598 and carbonation rate of alkaline industrial byproducts, *Constr. Build. Mater.*, 91,
599 216–224, <https://doi.org/10.1016/j.conbuildmat.2015.05.035>, 2015.
- 600 Trading Economics: Russia cement production, available at:
601 <https://tradingeconomics.com/russia/cement-production>, 2021
- 602 USEPA: Cement Kiln Dust Report to Congress, available at:
603 [https://archive.epa.gov/epawaste/nonhaz/industrial/special/web/html/cement2.ht](https://archive.epa.gov/epawaste/nonhaz/industrial/special/web/html/cement2.html)
604 [ml](https://archive.epa.gov/epawaste/nonhaz/industrial/special/web/html/cement2.html), 1993
- 605 Winter, C. and Plank, J.: The European dry-mix mortar industry (Part 1), *ZKG Int.*, 60,
606 62–69, 2007.
- 607 Xi, F., Davis, S. J., Ciais, P., Crawford-Brown, D., Guan, D., Pade, C., Shi, T., Syddall,
608 M., Lv, J., Ji, L., Bing, L., Wang, J., Wei, W., Yang, K.-H., Lagerblad, B., Galan,
609 I., Andrade, C., Zhang, Y., and Liu, Z.: Substantial global carbon uptake by cement
610 carbonation, *Nat. Geosci.*, 9, 880–883, <https://doi.org/10.1038/ngeo2840>, 2016.
- 611 Xu, J.-H., Fleiter, T., Eichhammer, W., and Fan, Y.: Energy consumption and CO₂
612 emissions in China’s cement industry: A perspective from LMDI decomposition
613 analysis, *Energ. Policy*, 50, 821–832, <https://doi.org/10.1016/j.enpol.2012.08.038>,
614 2012.
- 615 Xu, J.-H., Fleiter, T., Fan, Y., and Eichhammer, W.: CO₂ emissions reduction potential
616 in China’s cement industry compared to IEA’s Cement Technology Roadmap up
617 to 2050, *Appl. Energy*, 130, 592–602,
618 <https://doi.org/10.1016/j.apenergy.2014.03.004>, 2014.
- 619 Xuan, D., Zhan, B., Poon, C. S., and Zheng, W.: Carbon dioxide sequestration of
620 concrete slurry waste and its valorisation in construction products, *Constr. Build.*
621 *Mater.*, 113, 664–672, <https://doi.org/10.1016/j.conbuildmat.2016.03.109>, 2016.
- 622 Yang, K.-H., Seo, E.-A., and Tae, S.-H.: Carbonation and CO₂ uptake of concrete,
623 *Environ. Impact Assess. Rev.*, 46, 43–52,
624 <https://doi.org/10.1016/j.ear.2014.01.004>, 2014.



- 625 Yang, K.-H., Song, J.-K., and Song, K.-I.: Assessment of CO₂ reduction of alkali-
626 activated concrete, *J. Clean Prod.*, 39, 265–272,
627 <https://doi.org/10.1016/j.jclepro.2012.08.001>, 2013.
- 628 Yoon, I.-S., Çopuroğlu, O., and Park, K.-B.: Effect of global climatic change on
629 carbonation progress of concrete, *Atmos. Environ.*, 41, 7274–7285,
630 <https://doi.org/10.1016/j.atmosenv.2007.05.028>, 2007.
- 631 Zafeiropoulou, T., Rakanta, E., and Batis, G.: Performance evaluation of organic
632 coatings against corrosion in reinforced cement mortars, *Prog. Org. Coat.*, 72,
633 175–180, <https://doi.org/10.1016/j.porgcoat.2011.04.005>, 2011.
- 634 Zhou, H.: *Construction and Installation Engineering Budget Manual*, China Machine
635 Press, 2003.